

LASERS

PACS numbers: 42.55.Lt; 42.60.Lh
DOI: 10.1070/QE2005v035n12ABEH008963

Gain dynamics in the active medium of a pulsed e-beam sustained discharge CO laser: theory and experiment

S.V. Vetoshkin, A.A. Ionin, Yu.M. Klimachev, A.Yu. Kozlov, A.A. Kotkov, A.K. Kurnosov, A.P. Napartovich, O.A. Rulev, L.V. Seleznev, D.V. Sinitsyn, S.L. Shnyrev

***Abstract*. The small-signal gain (SSG) dynamics is studied experimentally and theoretically in the active medium of a pulsed e-beam sustained discharge CO laser in a broad range of vibrational transitions, various compositions and densities of the active medium, as well as various positions of a small-aperture probe laser beam in the gas-discharge region. The results of measurements are compared with theoretical calculations based on a spatially homogeneous CO laser model taking into account the multiquantum VV exchange processes. The sensitivity of the SSG dynamics to variations in the active medium and pump parameters is studied. Good agreement is demonstrated between theoretical and experimental data on the SSG dynamics obtained by using corrected values of local energy input in the calculations.**

Keywords: *kinetic model, multiquantum exchange, vibrational level, carbon monoxide, nonself-sustained discharge, active medium, CO laser*.

1. Introduction

The small-signal gain (SSG) dynamics in the active medium of a pulsed carbon monoxide e-beam sustained discharge (EBSD) laser sheds light on the processes of excitation of vibrational levels of CO molecules and vibration – vibration (VV) exchange, as well as on the dynamics of propagation of an excitation wave in the plateau region of the vibrational distribution function (VDF) and the subsequent evolution of the quasi-stationary VDF [1 – 4]. The presence of a rather wide region with uniform distribution of plasma parameters in the EBSD facilitates the interpretation of the results of measurements. For other excitation techniques, the method of VDF reconstruction from the variation of intensity of spontaneous emission in the overtone band [5] is widely used, because the gain measurement is hampered by the small length of the uniformly excited region. The radial inhomogeneity of a plasma introduces a considerable uncertainty in a low-pressure self-sustained discharge [6], while in the case of optical pumping by a focused beam [7] both the radius and length of the medium being excited are small, i.e., the density and temperature gradients are large [8]. The nonself-sustained EBS discharge in a chamber with a large volume of the discharge region and a wide aperture allows the SSG measurement by a small-aperture laser beam away from the discharge edges, i.e., under conditions of the most homogeneous active medium. In this case, the measurement of the SSG dynamics provides the time-resolved local diagnostics.

It was shown in [9 – 13] that for a more correct description of the vibrational kinetics and heating of the active medium of a CO laser, a model of VV-multiquantum exchange (MQE) should be used instead of the normally employed single-quantum VV-exchange model. However, for vibrational levels with $v > 15$, the absence of experimental data about the rate constants of VV exchange necessitates the use of the results of theoretical calculations (see, for example, [12, 13]). Therefore, a comparison of the theory with the experiments on the amplification of radiation on transitions between such levels is quite significant. From this point of view, it must be noted that the experimental data on the gain dynamics contain much more information than the data on energy and spectral parameters of the CO laser radiation (see, for example, [11, 14]) which, as a rule, are integrated and averaged.

In this study, the gain dynamics is theoretically investigated by using the MQE model with the VV-exchange rate constants [12, 13] calculated by using the semiclassical theory of collisions. The aim of this work is to compare the theoretical SSG dynamics with the experimental results. Such a comparison makes it possible to verify the applicability of the kinetic model used by us for describing the processes occurring in the active medium of a EBSD CO laser. We measured the SSG dynamics for a large number of vibration – rotation transitions (including transitions with $v > 15$) for different parameters of the active medium and pump pulses. We also discuss the extent to which the gain dynamics depends on such local parameters as the specific energy input and translational temperature of the gas.

2. Experimental setup

The gas mixture was pumped by a pulsed nonself-sustained EBS discharge in a discharge chamber with cryogenic cooling [4]. The average gas temperature T_0 in the discharge

S.V. Vetoshkin, A.A. Ionin, Yu.M. Klimachev, A.Yu. Kozlov, A.A. Kotkov, L.V. Seleznev, D.V. Sinitsyn P.N. Lebedev Physics Institute, Russian Academy of Sciences, Leninskii prosp. 53, 119991 Moscow, Russia; e-mail: aion@sci.lebedev.ru;

A.K. Kurnosov, A.P. Napartovich, O.A. Rulev, S.L. Shnyrev Federal State Unitary Enterprise, State Research Centre of Russian Federation 'Troitsk Institute for Innovation and Fusion Research', 142190 Troitsk, Moscow region, Russia; e-mail: apn@triniti.ru

Received 28 April 2005; revision received 4 October 2005
Kvantovaya Elektronika **35** (12) 1107 – 1112 (2005)
Translated by Ram Wadhwa

chamber of volume ~ 160 L was ~ 100 K. Since the gas was cooled through the walls of the discharge chamber, the distribution of the gas temperature T before pumping was nonuniform, the temperature increasing from 77 K (lower wall of the chamber) to ~ 140 K (upper flange and the foil separating the chamber from the electron accelerator). The separation H between the electrodes at the centre of the discharge region was 90 mm. The geometrical volume of the discharge region was $V_0 = HDL \approx 17.8$ L, where $L = 1.2$ m is the length and $D = 165$ mm is the width of this region. The distribution of the initial gas temperature in the volume between the electrodes was measured by a thermocouple probe and the results of measurements are presented in Fig. 1. For the gas mixture CO : He = 1 : 4, the gas temperature in the middle of the region between electrodes was 110 K, while for the gas mixture CO : N_2 = 1 : 9, it was 120 K. The temperature gradient along the height of the discharge gap was ~ 4 K cm^{-1} for the gas mixture CO : He = 1 : 4 and ~ 3 K cm^{-1} for the gas mixture CO : N_2 = 1 : 9 (for comparison, the temperature nonuniformity in a self-sustained discharge may exceed 100 K cm^{-1} [6]). In the vicinity of the warm output windows, the gas temperature along the axis of the discharge gap near the electrode edges is 5 K higher than in the middle of the discharge region.

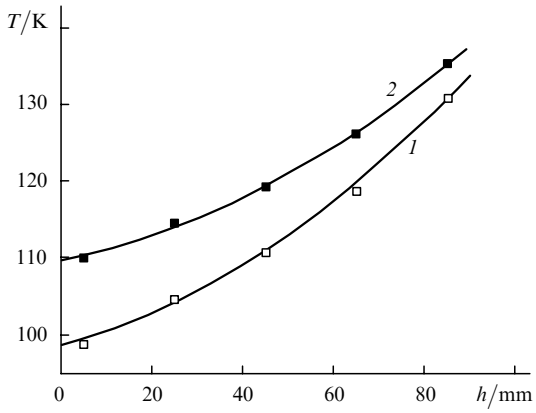

Figure 1. Distribution of the initial gas temperature T over the height h of the interelectrode gap at the middle of the discharge chamber for the mixtures CO : He = 1 : 4 (*1*) and CO : N_2 = 1 : 9 (*2*) for the average gas temperature $T_0 = 100$ K in the discharge chamber and the average gas density $N_0 = 0.12$ amagat.

The gas in the discharge chamber was ionised by a 150-keV electron beam. Because the current density of the electron beam varies along the height of the discharge gap due to scattering of electrons by the grid cathode of the discharge chamber and in the dividing foil, by using Faraday caps [15] we performed probe measurements of the electron flux density in the beam through a horizontal plane parallel to the plane of the lower electrode (anode). Figure 2 shows the results of measurements in the form of the distribution profiles at half the width d of the discharge region at various distances h from the anode. The highest (peak) current density ~ 20 mA cm^{-2} of the electron beam was measured near the grid cathode ($h = 76$ mm).

Pumping of the active medium of a pulsed gas-discharge laser is characterised by the specific energy input (SEI). In the experiments, the total energy supplied to the EBS discharge was determined by measuring the initial (U_1) and final (after the passage of the pumping pulse) voltage (U_2) across a battery of capacitors with a capacitance $C_0 \approx 53$ μF. The specific energy input averaged over the volume V_0 of the discharge region was estimated as $Q_{in} = C_0(U_1^2 - U_2^2)(2V_0N_0)^{-1}$, where N_0 is the average gas density in the discharge chamber. The relative gas concentration at the cryogenic temperature can be presented in amagat, the density of the gas N_0 (in amagat) is numerically equal to the number of moles of the gas in a molar volume (22.4 L), while SEI is expressed in J L^{-1} amagat^{-1} (1 J L^{-1} amagat^{-1} = 22.4 J mole^{-1}).

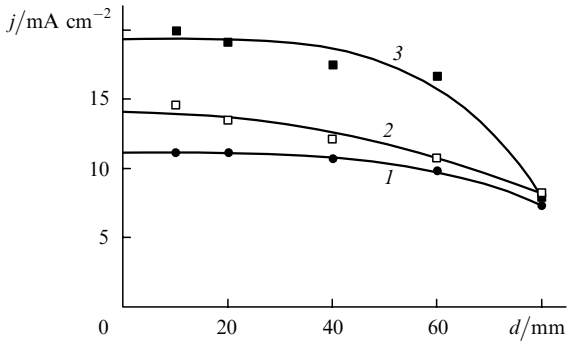

Figure 2. Electron beam current density j measured in vacuum at a distance d from the EIL axis in the discharge chamber for $h = 7$ (*1*), 46 (*2*) and 76 mm (*3*).

The time dependence of the pump power is of considerable importance for interpreting the SSG dynamics. In order to determine this dependence, we must know the pulse shape of the EBS discharge current $I(t)$ (Fig. 3a), which was measured with a bifilar low-inductance shunt, as well as the pulse shape of the discharge voltage $U(t)$ (Fig. 3b), which was measured with a resistive-capacitive divider. The onset of the signals was obscured by the high-frequency noise arising in the leading edge of the pump pulse. Figure 3c shows the pulse shape of the EBS discharge power $W(t) = U(t)I(t)$. The pump-pulse duration measured at the 0.1 level of the maximum power was 40 μs, almost coinciding with the pulse duration of the EBS discharge current (see Fig. 3a).

The above measurements were used to determine the spatially local parameters of the active medium (initial temperature and the corresponding gas density, current density of the electron beam and the pump-power dynamics) which are required for a correct analysis of the experimental data on the SSG dynamics and for comparing them with the results of theoretical calculations.

The SSG dynamics in the active medium of a pulsed EBSD CO laser was measured by the laser probing technique (the method of SSG measurement was described in detail in [4]). The error in SSG measurements varied from 2 % to 10 % of its maximum value. A specially designed frequency-selective low-pressure cw laser with cryogenic cooling was used for probing [4]. Cooling was required for the emission spectrum of this laser to cover the vibration–rotation transitions with the highest gain in the investigated medium with a gas temperature ~ 100 K. The use of such a probe laser with a beam diameter ~ 10 mm allows a spatially local diagnostics of the SSG dynamics in a broad range of vibration–rotation transitions under various pump conditions of the active medium of a wide-aperture pulsed EBSD CO laser.

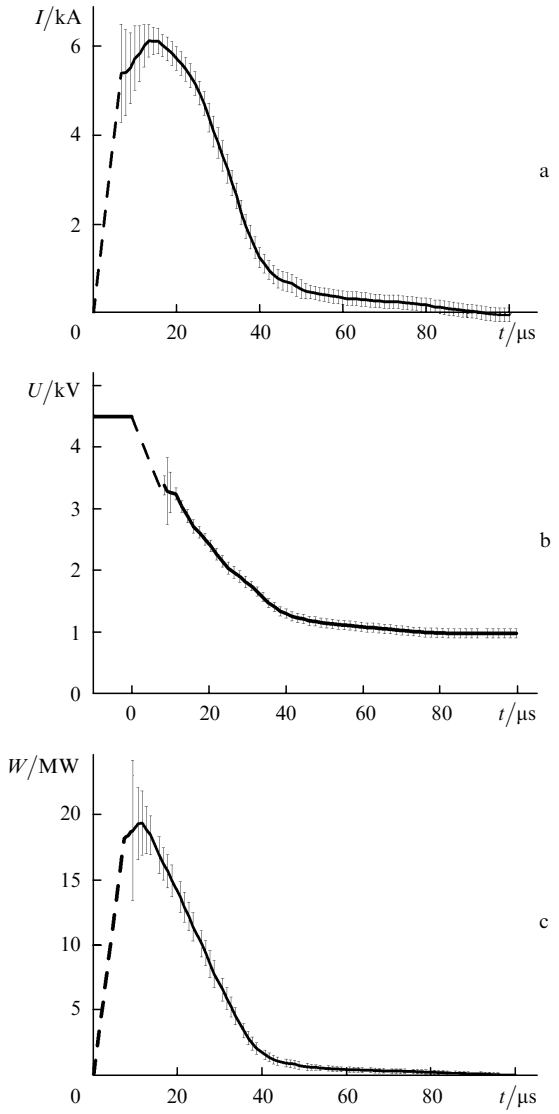

Figure 3. Shapes of the current I (a), voltage U (b) and pump power $W = UI$ (c) pulses in the EBS discharge for the CO : N_2 = 1 : 9 mixture, $Q_{in} = 250$ J L^{-1} amagat^{-1}, $T_0 = 100$ K and $N_0 = 0.12$ amagat.

3. Theoretical model

The theoretical model of the population dynamics of individual vibrational levels is described in [10, 13] and includes processes of excitation and de-excitation of molecules by electron impact, multiquantum VV exchange and VT relaxation, as well as spontaneous and induced emission.

The multiquantum exchange (MQE) model [12, 13] takes into account the VV-exchange processes between CO molecules (the number of quanta being exchanged varies from one to four) and the nonsymmetric VV exchange between highly excited and unexcited carbon monoxide molecules: $CO(v) + CO(0) \rightarrow CO(v-2) + CO(1) + \Delta E$, (where ΔE is the energy defect of the reaction), as well as the nonsymmetric VV$'$ exchange between CO and N_2 molecules.

The system of vibrational kinetics equations in the MQE model was solved together with the stationary Boltzmann equation for the electron energy distribution function (EEDF). The numerical solution of the Boltzmann equation for CO – He and CO – N_2 mixtures took into account all the fundamental processes of inelastic scattering of electrons from molecules, including scattering of electrons from vibrationally excited molecules (see [16] for details). The Boltzmann equation was solved with a time step determined by the rate of variation in the parameters monitored in calculations (the reduced field strength E/N and population density of the first vibrational level). In the numerical solution of the Boltzmann equation for the EEDF, the total energy balance of electrons was monitored and maintained with an error not exceeding 1 %.

A change in the density of the active medium affects the VDF and SSG dynamics. Under experimental conditions, the excited gas was expanded in a buffer volume, which was much larger than the active medium volume. This effect was taken into account in calculations of the SSG dynamics in the same way as in [3].

To analyse the sensitivity of the calculation results to the exact values of the parameters of the active medium and its pumping, numerical simulation of the SSG dynamics was performed by varying the SEI and the initial gas temperature. Calculations were performed for the CO : He = 1 : 4 mixture with the density $N_0 = 0.12$ amagat for local SEI values $Q_0 = 70 - 150$ J L^{-1} amagat^{-1}. The initial reduced field strength E/N in the middle of the discharge region in this case was $(1.0 - 1.5) \times 10^{-16}$ V cm^2. The current and voltage pulse shapes obtained in the experiments for a pump-pulse duration of 40 μs at the 0.1 level of the maximum power were used in calculations (see Fig. 3).

Figure 4 shows the SSG dynamics at the $10 \rightarrow 9\,P(9)$ transition, calculated for three values of SEI, other parameters remaining the same. The time dependence of SSG varies considerably upon variation of SEI. A comparison of the theoretical and measured SSG dynamics allows one to estimate Q_0 in the active medium region being probed.

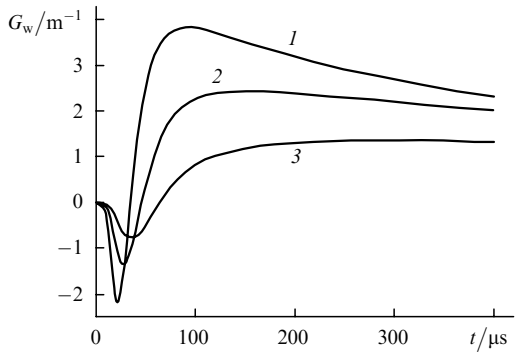

Figure 4. The SSG dynamics G_w at the $10 \rightarrow 9\,P(9)$ transition calculated for the CO : He = 1 : 4 mixture for $Q_0 = 150$ (*1*), 100 (*2*), and 70 J L^{-1} amagat^{-1} (*3*), $T_0 = 110$ K and $N_0 = 0.12$ amagat.

The SSG dynamics was calculated for $Q_0 = 70$ J L$^{-1}\times$ amagat^{-1} for different initial gas temperatures (Fig. 5). Note that the SSG amplitudes are extremely sensitive to the initial temperature. The increase in the gas temperature by 20 K (from 100 to 120 K) reduces the SSG amplitude by a factor of ~ 1.8. Therefore, to analyse the SSG dynamics, it is important to know the local initial gas temperature.

Thus, it is shown that the SSG dynamics is quite sensitive to the initial translational temperature and to the local value of the SEI. The distribution of the initial

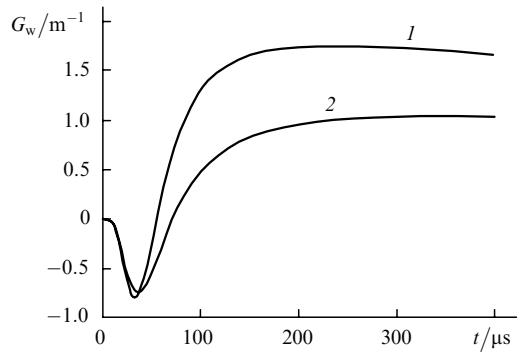

Figure 5. The SSG dynamics G_w at the $10 \rightarrow 9\,P(9)$ transition calculated for the CO : He = 1 : 4 mixture for the initial temperature $T = 100$ (*1*), 120 K (*2*) of the medium, $Q_0 = 70$ J L^{-1} amagat^{-1} and $N_0 = 0.12$ amagat.

temperature (and gas density) and the pump-pulse shape were quite reliably determined in our experiments. As for the SEI, only approximate values of Q_{in} were determined in the experiments. An analysis of the experimental data (Fig. 2) on the current density of an electron beam and of the discharge chamber configuration used in our experiments allowed us to estimate the local values of SEI, which were found to be $(0.7 \pm 0.1)Q_{in}$ in the interelectrode region. Note that an additional uncertainty in the values of the voltage drop in the near-electrode layers (see, for example, [17]) makes such an estimate quite unreliable; hence we used an alternative approach. Taking into account a strong effect of the SEI on the SSG dynamics (Fig. 4), the local SEI value Q_0 was used as the variable parameter of the model. The required value of Q_0 was determined from the condition of the best fit of experimental data.

4. Experimental data and their comparison with the results of calculations

Consider the results of SSG measurements performed for different distances h from the axis of the probe laser beam (of diameter 10 mm) to the surface of the lower electrode (anode). Measurements were made in the vertical plane passing through the centre of the discharge region ($d = 0$ in Fig. 2). Figure 6 shows the experimental data obtained for the $20 \rightarrow 19\,P(12)$ transition in the CO : He = 1 : 4 mixture for $Q_{in} = 105$ J L^{-1} amagat^{-1} at distances $h = 14$, 34 and 57 mm, corresponding to the initial gas temperatures of 102, 107 and 116 K. The figure also shows the results of calculations. The observed SSG variations caused by changes in the probe-beam position are mainly explained by differences in the initial temperatures and gas densities. The local SEI values for which a satisfactory agreement between the theory and experiment was achieved for different h do not differ significantly from one another and amount to about $0.7Q_{in}$. This suggests that the spatial inhomogeneity of the local SEI in the region of the active medium being probed is small. Such a conclusion agrees with the results of measurements of the energy input distribution in the EBS discharge [18]. Subsequent SSG measurements were mainly performed for $h = 35 \pm 2$ mm.

The experimental SSG dynamics in the CO : He = 1 : 4 mixture for the average gas density $N_0 = 12$ amagat and $Q_{in} = 150$ J L^{-1} amagat^{-1} measured for six vibrational transitions (from $11 \rightarrow 10$ to $21 \rightarrow 20$) is compared with

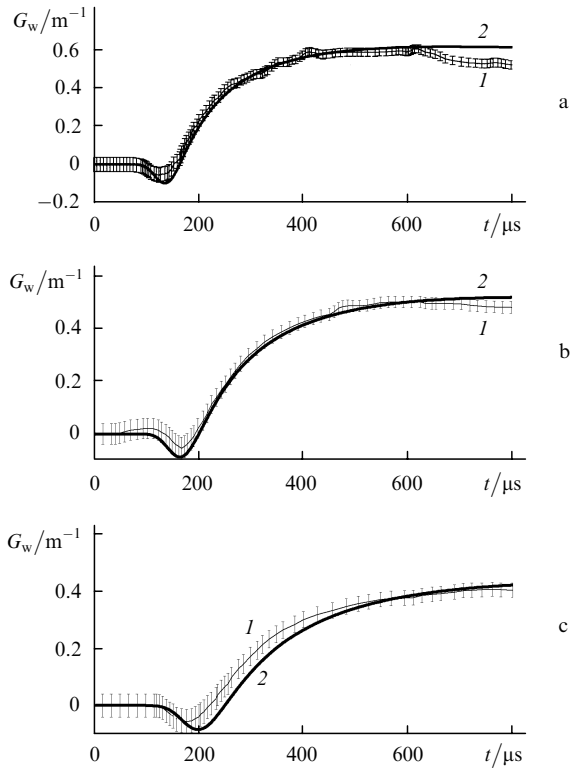

Figure 6. Comparison of the experimental (*1*) and theoretical (*2*) data on the SSG dynamics G_w at the $20 \rightarrow 19\,P(12)$ transition for the CO : He = 1 : 4 mixture for $h = 14$ (a), 34 (b) and 57 mm (c); $Q_0 = 70$ J L^{-1} amagat^{-1}, $Q_{in} = 105$ J L^{-1} amagat^{-1}, $T_0 = 100$ K and $N_0 = 0.12$ amagat.

calculations in Fig. 7. A reasonably good agreement with the theory is achieved for $Q_0 = 94$ J L^{-1} amagat^{-1} = $0.63Q_{in}$. Such a value of Q_0 allows a satisfactory interpretation of the experimental data on the SSG dynamics not only in a broad range of vibrational transitions, but also for various densities of the active medium of the CO : He = 1 : 4 composition. This is illustrated in Fig. 8 in which the experimentally measured SSG dynamics at the transition $19 \rightarrow 18\,P(14)$ for a density 0.06 amagat of the medium is compared with calculations.

For the nitrogen-containing mixture CO : N_2 = 1 : 9, the local value of the SEI was also determined from the condition of the best fit of experimental results by the calculated SSG dynamics. As for the helium mixture CO : He = 1 : 4, the obtained values of Q_0 were found to be much smaller than Q_{in}. The results of SSG measurements in the CO : N_2 = 1 : 9 mixtures for $Q_{in} = 250$ J L^{-1} × amagat^{-1} are compared in Fig. 9 with the results of calculations ($Q_0 = 180$ J L^{-1} amagat^{-1} = $0.72Q_{in}$). The comparison was performed for five vibration–rotation transitions: $13 \rightarrow 12\,P(9, 15)$, $16 \rightarrow 15\,P(10, 14, 16)$. Such a reasonable agreement between the theory and experiment in the CO–N_2 mixture is obtained for a smaller correction of the SEI than in the CO–He mixture, which can be explained by a slightly slower rate of heating of the nitrogen-containing mixture.

Note that there are a number of constraints on the applicability of the spatially homogeneous theoretical model used by us for describing experimental data on the SSG dynamics for large SEI values (more than 300 J L^{-1} × amagat^{-1} for the CO–He mixture and more than

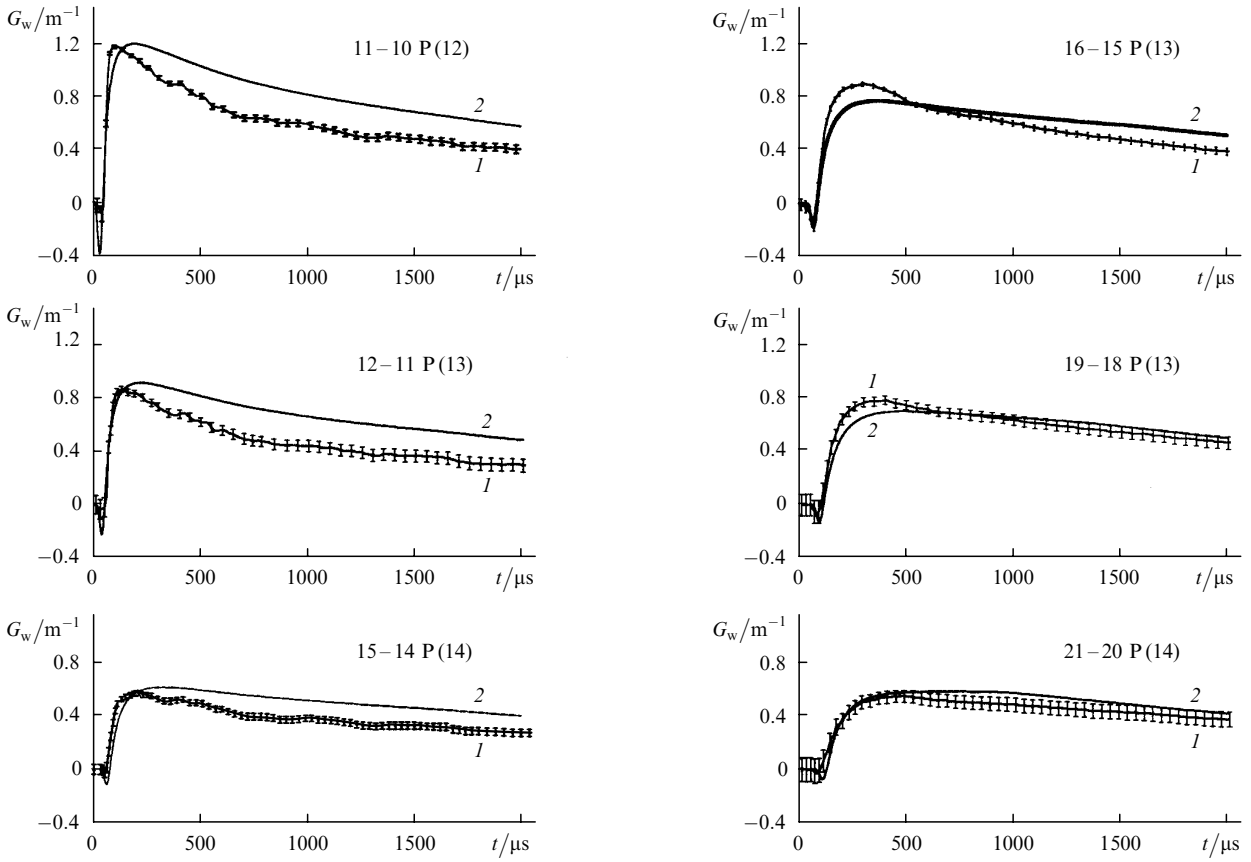

Figure 7. The SSG dynamics G_w at six vibrational transitions for the CO : He = 1 : 4 mixture for $N_0 = 0.12$ amagat and $T_0 = 100$ K. The experimental data (*1*) correspond to $Q_{in} = 150$ J L^{-1} amagat^{-1}; the theoretical dependences (*2*) were calculated for $Q_0 = 94$ J L^{-1} amagat^{-1}.

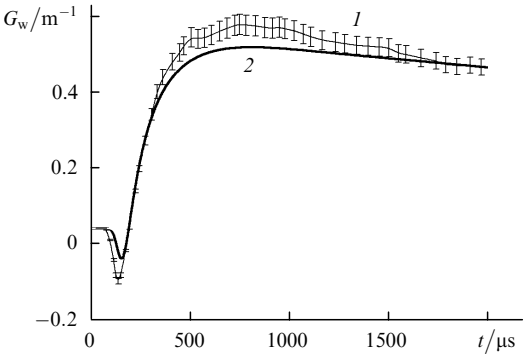

Figure 8. The SSG dynamics G_w for the 19 → 18 P(14) transition for the CO : He = 1 : 4 mixture for $N_0 = 0.06$ amagat and $T_0 = 100$ K. The experimental data (*1*) correspond to $Q_{in} = 150$ J L^{-1} amagat^{-1}; the theoretical dependences (*2*) were calculated for $Q_0 = 94$ J L^{-1} amagat^{-1}.

400 J L^{-1} amagat^{-1} for the CO–N_2 mixture). For such SEI values, the theoretical model is in agreement with experiments at times that are short compared to the characteristic gas-dynamic times. An explanation of this effect is beyond the framework of the spatially homogeneous model of the active medium. This effect is probably explained by the formation of compression and rarefaction waves due to nonuniform heat release in the active medium [19, 20].

5. Conclusions

We have measured the SSG dynamics in the active medium of a pulsed EBSD CO laser for various parameters of the

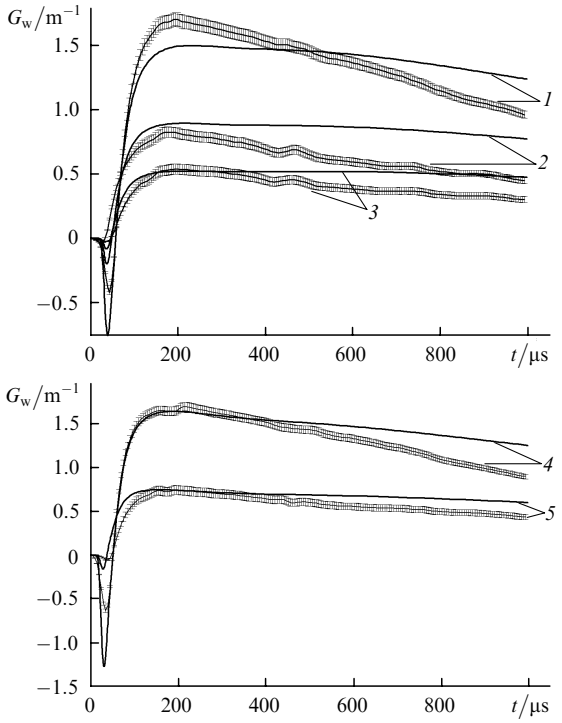

Figure 9. The SSG dynamics G_w at the vibration–rotation transitions 16 → 15 P(10) (*1*), 16 → 15 P(14) (*2*), 16 → 15 P(16) (*3*), 13 → 12 P(9) (*4*), and 13 → 12 P(15) (*5*) for the CO : He = 1 : 4 mixture for $N_0 =$ 0.12 amagat and $T_0 = 100$ K. The experimental data are shown with the measuring error and correspond to $Q_{in} = 250$ J L^{-1} amagat^{-1}; the theoretical dependences were calculated for $Q_0 = 180$ J L^{-1} amagat^{-1}.

medium and pump pulses in a broad range of vibration–rotation transitions (including transitions for $v > 15$). The theoretical model developed by us satisfactorily describes the SSG dynamics as a whole. Agreement with the experimental data was observed in a broad range of vibrational transitions at different densities and different compositions of the active medium, which points not only to the reliability of the set of VV-exchange constants used by us, but also to a correct determination of the active medium and pump parameters obtained in the experiments.

Acknowledgements. This work was supported by the Russian Foundation for Basic Research (Grant No. 02-02-17217), International Scientific and Technology Centre (Grant No. 2415-P), and a grant from the President of Russian Federation (No. RI-112-001-593).

References

1. Boness M.J.W., Center R.E. *Appl. Phys. Lett.*, **26**, 511 (1975).
2. Basov N.G., Kazakevich V.S., Kovsh I.B., Mikryukov A.N. *Kvantovaya Elektron.*, **10**, 1049 (1983) [*Sov. J. Quantum Electron.*, **13**, 667 (1983)].
3. Basov N.G., Ionin A.A., Klimachev Yu.M., et al. *Kvantovaya Elektron.*, **32**, 404 (2002) [*Quantum Electron.*, **32**, 404 (2002)].
4. Vetoshkin S.V., Ionin A.A., Klimachev Yu.M., et al. *Preprint FIAN*., (13) (Moscow, 2005).
5. Lightman A.J., Fisher E.R. *J. Appl. Phys.*, **10**, 971 (1978).
6. Grigoryan G.M., Ionikh Y.Z., Kochetov I.V., et al. *J. Phys. D*, **25**, 1064 (1992).
7. Flament C., George T., et al. *Chem. Phys.*, **163**, 241 (1992).
8. Kochetov I.V., Kurnosov A.K., Martin G.P., Napartovich A.P. *Kvantovaya Elektron.*, **22**, 683 (1995) [*Quantum Electron.*, **25**, 655 (1995)].
9. Ionin A.A., Klimachev Yu.M., Konev Yu.B., et al. *Izv. Ross. Akad. Nauk, Ser. Fiz.*, **63**, 676 (1999).
10. Ionin A.A., Klimachev Yu.M., Konev Yu.B., et al. *Kvantovaya Elektron.*, **30**, 573 (2000) [*Quantum Electron.*, **30**, 573 (2000)].
11. Basov N.G., Ionin A.A., Kotkov A.A., et al. *Kvantovaya Elektron.*, **30**, 859 (2000) [*Quantum Electron.*, **30**, 859 (2000)].
12. Billing G.D., Coletti C., Kurnosov A.K., Napartovich A.P. *J. Phys. B: At. Mol. Opt. Phys.*, **36**, 1175 (2003).
13. Cacciatore M., Kurnosov A., Napartovich A., Shnyrev S. *J. Phys. B: At. Mol. Opt. Phys.*, **37**, 3379 (2004).
14. Basov N.G., Ionin A.A., Kotkov A.A., et al. *Kvantovaya Elektron.*, **30**, 771 (2000) [*Quantum Electron.*, **30**, 771 (2000)].
15. Vetoshkin S.V., Ionin A.A., Klimachev Yu.M., et al. *Preprint FIAN.*, (27) (Moscow, 2004).
16. Kochetov I.V., Kurnosov A.K., Napartovich A.P., Shnyrev S.L. *Fiz. Plazmy*, **28**, 1128 (2002).
17. Raizer Yu.P. *Fizika Gazovogo Razryada* (Physics of Gas Discharge) (Moscow: Nauka, 1987).
18. Boiko E.S., Minin V.V., Tret'yakov V.E., Yatsenko B.P. *Preprint NIIEFA P-A-0530* (Leningrad, 1981).
19. Basov N.G., Dolinina V.I., Zvorykin V.D., et al. *Preprint FIAN.*, (292) (Moscow, 1983).
20. Aliev E.T., Basov N.G., Kovsh I.B., et al. *Kvantovaya Elektron.*, **11**, 874 (1984) [*Sov. J. Quantum Electron.*, **14**, 593 (1984)].